Volume 4, Issue 7, July 2014 ISSN: 2277 128X

International Journal of Advanced Research in Computer Science and Software Engineering

Research Paper

Available online at: www.ijarcsse.com

Numerical Study of Optical Properties of Tow Assembled Gold-Core/Polymer-Shell Nanoparticles in Dielectric Medium

A. Akouibaa
Polymer Physics and Critical Phenomena Laboratory.
Research Center Materials And Energy.
Sciences Faculty Ben M.Sik, P.O. BOX 7955, Casablanca, Morocco

A. Derouiche
Polymer Physics and Critical Phenomena Laboratory.
Research Center Materials And Energy.
Sciences Faculty Ben M.Sik, P.O. BOX 7955, Casablanca, Morocco

H. Ridouane
Polymer Physics and Critical Phenomena Laboratory.
Research Center Materials And Energy.
Sciences Faculty Ben M.Sik, P.O. BOX 7955, Casablanca, Morocco

A. Bettachy
Polymer Physics and Critical Phenomena Laboratory.
Research Center Materials And Energy.
Sciences Faculty Ben M.Sik, P.O. BOX 7955, Casablanca, Morocco

F. Benzouine
Polymer Physics and Critical Phenomena Laboratory.
Research Center Materials And Energy.
Sciences Faculty Ben M.Sik, P.O. BOX 7955, Casablanca, Morocco

Abstract— Recently, the polymer modified gold nanoparticles have showed much potential in advanced materials. In this paper we have used the finite element method (FEM) for the calculation of the effects coupling on the plasmonic resonances of the gold-core/polymer-shell nanospheres. Several plasmonics structures have dimensions much smaller than the wavelength of the incident light. Under these conditions, retardation effects are negligible and the field distribution problem then reduced to solve Laplace's equation. The study is performed for various possible configurations of two coated gold nanoparticles (GNPs) when they are aggregating in dielectric medium. The numerical results that we have obtained show that the absorption spectrum of coupled coated-GNPs is depending to the polymer-shell thickness, the nature of the polymer constituting the shell and the gold-core radius.

Keywords—coated gold nanoparticles, polymers shells, optical properties, surface plasmon resonance, finite element method

I. INTRODUCTION

In recent years, gold nanoparticles have been extensively studied and used in various applications because of their unique optical and catalytic properties (e.g. [1]–[12]). The optical properties are due to electron oscillations in the metallic particles induced by the incident light field, giving rise to the so-called surface plasmon resonance (SPR) (e.g. [1]–[5]). The efficiency of gold nanoparticles (GNPs) to absorb and scatter light is highly dependent on the size and the shape of the GNP and on the dielectric properties of the environment (e.g. [5], [13]). The surface plasmon oscillation in metallic nanoparticles is drastically changed if the particles are densely packed in the dielectric medium, so that the individual particles are electronically coupled to each other. It was found theoretically and experimentally that when the individual spherical gold nanoparticles come into close proximity the one to another, electromagnetic coupling of nanoparticles becomes efficient for interparticles distances smaller than five times the nanoparticle radius ($d \leq 5R$ where, d is the center-to-center distance and R is the radius of the particles). In addition, the effect coupling lead to complicated extinction spectra depending on the size and shape of the formed cluster aggregate by the splitting of single cluster resonance. (e.g. [14]-[18]) Aggregation causes a coupling of the gold nanoparticles plasmon modes, which results in a red shift and broadening of the longitudinal plasma resonance in the optical spectrum. (e.g. [19]) The wavelength at which absorption due to dipole-dipole interactions occurs may be varied from 520 nm (effectively isolated particles) through 750 nm (particles that are separated by only 0.5 nm), and the resulting spectra are a composite of the conventional plasmon resonance due to single spherical particles and the new peak due to particle-particle interactions. (e.g. [20]-[24]).

Gold nanoparticles are colloidally unstable and are susceptible to irreversible aggregation. To stabilize them, they can be coated with small organic molecules such as citrates, surfactants, ligands or polymers. Schiffrin and *coworkers* (e.g. [25]) reported the two-phase reduction method to produce alkanethiolate-protected gold nanoparticles with tunable particle size between 1nm to 10nm depending on the ratio of the Au salt and the alkanethiol ligand.

Functional ligands can also be attached to the nanoparticle surface to provide an additional tool to design surface architecture and to modulate physico-chemical properties for compatibility and detection. To this end, polymeric ligands have proved to be a popular choice due to their flexibility for tailoring specific uses and also for their greater long-term stabilizing properties compared to small molecules such as citrates. Notable examples include polysaccharides (e.g. [26]), DNA (e.g. [27]-[31]) and a category of "smart" polymers (e.g. [32]) that possesses stimuli-responsive attributes, in particular, pH, salinity and temperature-sensitive polymers have been widely studied due to their potential applications in biomedical and delivery systems (e.g.[33]-[37]). Two ways of polymeric stabilization are distinguished: The "grafting-to" technique requires pre-synthesized polymers end-capped with a thiol (e.g. [38]-[40]), or dithioester (e.g. [41]), and polymers with disulphide unit (e.g. [42], [43]). In "grafting-from" method (e.g. [43]-[45]), monomers are polymerized from the surfaces carrying polymerization-initiating species. Both methods preferably involve controlled/living radical polymerization techniques such as ATRP (e.g. [46],[47]) and RAFT (e.g. [48]-[56]) to obtain a monodisperse and dense polymeric shell around the gold cores. We can cite a few examples of gold (e.g. [57]) and silver [58] nanoparticles grafted with RAFT thermo-sensitive polymers. Recent advances on synthesis and applications of polymer-protected gold nanoparticles can be found in a comprehensive review by Shan *et al* (e.g. [59]).

An original way to generate aggregation of GNPs consists in grafting on their surface stimuli-responsive polymers (e.g. [60]-[64]). Such polymers are chosen for the ability to change their conformation in response to an external stimulus such as pH, temperature or light. This gives them the ability to control individual systems. In concept, the stimuli-responsive polymers are also known as “environmentally sensitive” polymers (e.g. [65]-[67]), which will undergo relatively large and abrupt, physical or chemical changes as responses to small external stimuli in the environmental conditions (e.g. [68]-[71]). For polymers, the temperature and pH stimuli have been widely studied due to the reversibly responsive features. The stimuli response of the polymer chains can be intrinsically ascribed to the polymer solubility in different environments. In the Flory–Huggins theory, the solubility of polymer chains depends on the segment–solvent interaction which is defined by solvent quality (e.g. [72], [73]). Originally, the polymer brush chains are fully extended in solution. However, when adding an external stimulus they will collapse onto the solid cores densely and hence change the spatial occupation and surface property (e.g. [74]-[76]) .The inter-chains collapse results in the formation of aggregates of nanoparticles.

Numerical techniques are designed to solve the relevant filed equation in the computational domain, subject to the boundary constraints imposed by the geometry. Without making a priori assumption about which field interaction are most significant, numerical techniques analyze the entire geometry provided as input. The finite element method (FEM) (e.g. [77-78]), which is a powerful numerical modeling tool, has been widely used for modeling electromagnetic wave interaction with complex materials. As already mentioned, the computer simulation model based on FEM we develop here, was applied to three-dimensional systems. In this paper, we use this approach for computing the potential distribution in the composite material consisting of two coupled GNPs coated by Polymers and immersed in a dielectric medium and to derive its effective dielectric constant, this parameter allowed us to calculate the absorption cross-section. For this we used the core-shell model (gold-core/polymer-shell), the core and shell of particle and the environments are characterized by the dielectric constant. The main purpose of this work is to present various numerical results (in the quasi-static limit) of the absorption cross-section computed by FEM for a periodic composite structure in which the inclusions are the coupled gold nanoparticles coated with polymeric shell. The effect of several geometrical and physical parameters on the absorption spectrum are analyzed and compared.

II. EFFECTIVE DIELECTRIC PERMITTIVITY OF COMPOSITES WITH CORE-SHELL NANOPARTICLES

A two-phase nanoparticle is investigated in which spherical gold nanoparticles with interfacial polymeric shells are randomly embedded in a homogeneous matrix. Combining the interfacial shell and the gold core can be regarded as a ‘‘complex particle’’. Therefore, the three-phase random composite system can be regarded as the complex particles embedded in the matrix. For simplicity, the permittivity is assumed to be unchangeable inside the interfacial layer. We postulate that R_1 and R_2 are the radius of core with permittivity ε_1 and shell with permittivity ε_2 of the complex particle, respectively. The thickness of the shell is $e = R_1 - R_2$, and the permittivity of the matrix is ε_m. Under quasi- static approximation, when an electromagnetic field E_0 is incident perpendicularly to the complex particle, the electric potential in each component in composite is given by the Laplace equation (e.g. [79]):

$$\phi_c = -ArE_0 \cos\theta, \qquad r < R_1 \tag{1}$$

$$\phi_s = -E_0\left[Br - \frac{CR_1^3}{r^2}\right]\cos\theta, \qquad R_1 < r < R_2 \tag{2}$$

$$\phi_m = -E_0\left[r - \frac{DR_2^3}{r^2}\right]\cos\theta, \qquad R_2 < r \ (1) \tag{3}$$

Coefficients A, B, C and D are determined by the boundary conditions, respectively. As shown in Eq.(3), the outer electric potential contains two parts: one is the contribution of outfield and the second can be considered as the contribution of the electrical dipole moment of medium sphere. The overall electrical dipole moment of the spherical particle with polymeric shell is calculated through the electric potential generated by the electrical dipole moment in the space:

$$\vec{p} = \frac{\gamma\varepsilon_1 - \varepsilon_m}{\gamma\varepsilon_1 + 2\varepsilon_m} 4\pi\varepsilon_m R_2^3 \overrightarrow{E_0}, \tag{4}$$

Where:

$$\gamma = \frac{\beta(1-2\beta) + 2f_s\beta(1-\beta)}{(1+2\beta) - f_s(1-\beta)}, \tag{5}$$

With the volume ratio $f_s = R_1^3/R_2^3$ and equivalent coefficient $\beta = \varepsilon_2/\varepsilon_1$.

We note that in the case where there is no shell, that is $R_2 = R_1$ and $\beta = 1$, the above parameter reduces to $\gamma = 1$, the electrical dipole moment of the solid particle is calculated with the following formula:

$$\vec{p} = \frac{\varepsilon_1 - \varepsilon_m}{\varepsilon_1 + 2\varepsilon_m} 4\pi\varepsilon_m R_1^3 \overrightarrow{E_0}, \quad (6)$$

The effective medium theory and the Maxwell–Garnett theory are usually regarded as a convenient method to deal with the linear response of such a homogeneous composite system according to its microstructure (e.g. [80], [81]). The effective permittivity of the composite with single spherical inclusions is obtained from the average of polarization theory (e.g. [81]):

$$f\frac{\varepsilon_1 - \varepsilon_{eff}}{\varepsilon_1 + 2\varepsilon_{eff}} + (1 - f)\frac{\varepsilon_m - \varepsilon_{eff}}{\varepsilon_m + 2\varepsilon_{eff}} = 0, \quad (7)$$

Where f and $(1 - f)$ are the volume fractions of particles and matrix, respectively; ε_{eff} is the effective permittivity of composite; ε_1 and ε_m are the permittivity of filler particle and the matrix, respectively.

The effective permittivity of composite is given by Eq.(7) when only dipole interactions are present. For regular arrays this case occurs in the limit of low filling factor of scatter inclusions. However, higher multipole interactions become significant when particles approach contact, so Eq.(7) is inapplicable in regular arrays at high volume filling. In random or disordered distributions close encounters can occur at any volume filling, so higher multipole corrections are necessarily considered in disordered medium even at low volume filling. Furthermore, the higher multipole interactions intensify rapidly on enhancing the volume fraction of filler particles. In order to take the higher multipole interactions into account, we give a set of permittivity$(\varepsilon_1^b, \varepsilon_m^b)$ to replace the real permittivity$(\varepsilon_1, \varepsilon_m)$. The set of permittivity$(\varepsilon_1^b, \varepsilon_m^b)$ has something to do with permittivity$(\varepsilon_1, \varepsilon_m)$ and the shape of the particles. Based on the Maxwell–Garnett theory and the relation between two distinct topological structures (symmetry structure and dissymmetry structure) [81], ε_1^b and ε_m^b can be expressed as:

$$\varepsilon_1^b = \frac{2f}{3-f}\varepsilon_1 \quad (8)$$

$$\varepsilon_m^b = \frac{2(1-f)}{2+f}\varepsilon_m \quad (9)$$

Substituting Eqs. (8) And (9) into Eq. (7), we obtain the equation for the effective permittivity of two-phase randomly mixed composite:

$$f\frac{\varepsilon_1^b - \varepsilon_{eff}}{\varepsilon_1^b + 2\varepsilon_{eff}} + (1 - f)\frac{\varepsilon_m^b - \varepsilon_{eff}}{\varepsilon_m^b + 2\varepsilon_{eff}} = 0, \quad (10)$$

The following step investigates the composite containing core–shell spherical particles randomly distributed in a homogeneous matrix. Substituting in Eq (7) the permittivity ε_1 by the equivalent permittivity $\gamma\varepsilon_1$ we can get the equation for effective permittivity:

$$f'\frac{\gamma\varepsilon_1^b - \varepsilon_{eff}}{\gamma\varepsilon_1^b + 2\varepsilon_{eff}} + (1 - f')\frac{\varepsilon_m^b - \varepsilon_{eff}}{\varepsilon_m^b + 2\varepsilon_{eff}} = 0 \quad (11)$$

Where$f' = \frac{f}{f_s}$, and f is the volume fraction of core. The modified formula is universal and available for calculating effective permittivity of the composite system composed of coated spherical inclusion imbedded in homogeneous matrix randomly.

III. MODEL AND METHOD

3-1 method and characterization

In the past, nanoparticles grafted with polymers have been modelled with a few classic models (e.g. [82], [83]). In our study, the core-shell model is employed to characterize the protecting polymer shell, this model represents a sphere (the core gold) stacked in another sphere (the shell: polymer). The fitting geometrical parameters for this model are the gold core radius (R_c), the polymer shell radius (R_p) and the polymer shell thickness (e), $(e = R_p - R_c)$ as shown in Fig.1. The physical parameter characterizing the different phases of the nanocomposite is the dielectric permittivity (gold core ε_c, polymer shell ε_p and surrounding medium ε_m).

The dielectric constant of gold core is a function of frequency of the electromagnetic wave with which it interacts. Indeed, the interaction of an electromagnetic wave (with a pulse ω), with a metal will lead to a polarization of the medium. This polarization will then generate a change in the complex refractive index, $\tilde{n}(\omega)$, which is related to the dielectric constant by the following relationship:

$$\tilde{n}^2(\omega) = \varepsilon(\omega) \quad (12)$$

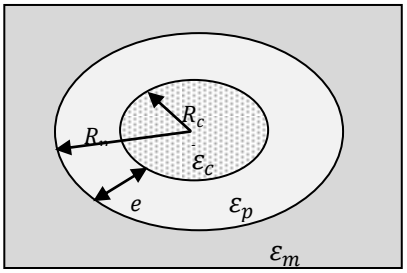

Fig. 1 Representation of the core-shell model

In order to describe the permittivity of Gold in a wide frequency band, use was made of two-critical points Drude model (two-CPDM) (e.g. [84]). This model is valid in the frequency band between 0.5eV to 6.5eV corresponding to wavelengths between 200nm and 2400nm. Within the framework of this model, the permittivity of a Gold nanoparticle is expressed by:

$$\varepsilon = \varepsilon_\infty - \frac{\omega_D^2}{\omega^2 + i\gamma\omega} + \sum_{j=1}^{2} A_j \Omega_j \left(\frac{e^{i\Phi_j}}{\Omega_j - \omega - i\Gamma_j} + \frac{e^{-i\Phi_j}}{\Omega_j + \omega + i\Gamma_j} \right) . \quad (13)$$

In this relationship, ε_∞ is the permittivity at infinite frequency, ω_D is the frequency of the volume plasmon, γ is the collision rate of electrons, and the third contribution in the r.h.s of the above relation represents the Lorentz term.

3-2 method

In this work we are interested in determining the effective dielectric permittivity of nanocomposite constituted by dimer gold nanoparticles coated with polymers immersed in a dielectric medium using the Finite-Element FE numerical tool. The detailed description of the method for determining the effective permittivity in the quasi-static limit can be found elsewhere (e.g. [85]). As both computing power and the efficiency of the FE computational method, it is becoming possible to investigate new composite materials through computer simulations before they have even been synthesized. FE tool is used to compute the solution of Laplace equation by determining the electric field and potential distribution from the physical properties of different phases of the composite material. Recent works have shown that the FE method could be successfully applied to compute the effective permittivity of periodic composite materials (e.g. [86]). The basic scheme of the FE method is now briefly recalled.

To describe the FEM scheme, we consider a spatial domain, Ω, shown in Fig.2 with a vanishing charge density. Solving the problem at hand means finding the local potential distribution inside the computational domain by solving Laplace's equation (first principal of electrostatic):

$$\vec{\nabla}\left(\varepsilon_0 \varepsilon(\vec{r}) \vec{\nabla} V(\vec{r})\right) = 0 , \quad (14)$$

Where $\varepsilon(r)$ and $V(\vec{r})$ are the local relative permittivity and the potential distribution inside the material domain respectively with zero charge density. $\varepsilon_0 = 8.85.10^{-12}\, F/m$ is the permittivity of the vacuum. In addition, the composite (dielectric) is assumed to be periodic with three phases (metallic core, polymeric shell and host matrix). Taking into account the symmetry and periodicity properties, the geometry of the medium is reduced to a unit cell. The implementation of the FE method consists in dividing the three-dimensional domain into tetrahedral finite elements and interpolating the potential V and its normal derivative $\frac{\partial V}{\partial n}$ on each finite element similarly to the BIE method (e.g. [87], [88]) with the corresponding nodal values:

$$V = \sum_i \lambda_i V_i \quad (15)$$

$$\frac{\partial V}{\partial n} = \sum_i \lambda_i \left(\frac{\partial V_i}{\partial n}\right) \quad (16)$$

Where λ_i denotes the interpolating functions.

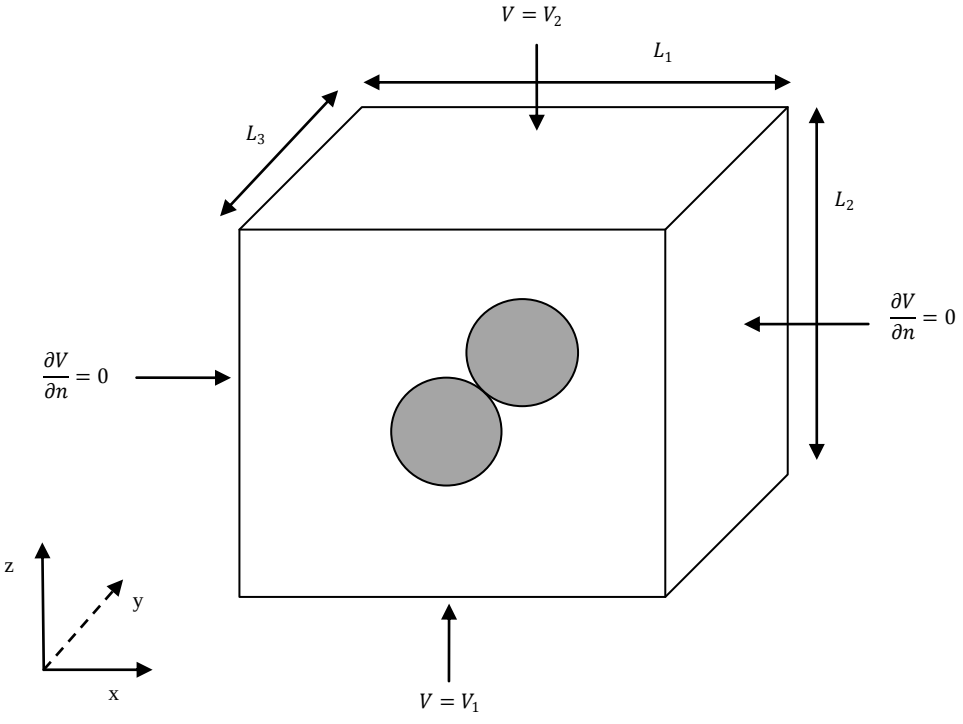

Fig. 2 Notation and boundary conditions related to a three-dimensional periodic nanocomposite. This cell contains two coupled coated gold nanoparticles

To describe the FEM scheme, we consider a spatial domain, Ω, shown in Fig.2 with a vanishing charge density. Solving the problem at hand means finding the local potential distribution inside the computational domain by solving Laplace's equation (first principal of electrostatic):

$$\vec{\nabla}\left(\varepsilon_0\varepsilon(\vec{r})\vec{\nabla}V(\vec{r})\right) = 0\,, \tag{14}$$

Where $\varepsilon(r)$ and $V(\vec{r})$ are the local relative permittivity and the potential distribution inside the material domain respectively with zero charge density. $\varepsilon_0 = 8.85.10^{-12}\,F/m$ is the permittivity of the vacuum. In addition, the composite (dielectric) is assumed to be periodic with three phases (metallic core, polymeric shell and host matrix). Taking into account the symmetry and periodicity properties, the geometry of the medium is reduced to a unit cell. The implementation of the FE method consists in dividing the three-dimensional domain into tetrahedral finite elements and interpolating the potential V and its normal derivative $\frac{\partial V}{\partial n}$ on each finite element similarly to the BIE method (e.g. [87], [88]) with the corresponding nodal values:

$$V = \sum_i \lambda_i V_i \tag{15}$$

$$\frac{\partial V}{\partial n} = \sum_i \lambda_i \left(\frac{\partial V_i}{\partial n}\right) \tag{16}$$

Where λ_i denotes the interpolating functions.

Following this analysis, the solution of Laplace's equation is obtained using the Galerkin method and by solving the resulting matrix equation from the boundary conditions thanks to a standard numerical technique, i.e., Gauss procedure (e.g. [77]).

Having computed the potential and its normal derivative on each tetrahedron of the computational mesh, the electrostatic energy W_e^k, and losses, P_e^k could be expressed for each tetrahedral element as:

$$W_e^k = \frac{\varepsilon_0}{2}\iiint_{V_k}\varepsilon_k'(x,y,z)\left[\left(\frac{\partial V}{\partial x}\right)^2 + \left(\frac{\partial V}{\partial y}\right)^2 + \left(\frac{\partial V}{\partial z}\right)^2\right]dV_k\,, \tag{17}$$

$$P_e^k = \frac{\varepsilon_0}{2}\iiint_{V_k}\omega\varepsilon_k''(x,y,z)\left[\left(\frac{\partial V}{\partial x}\right)^2 + \left(\frac{\partial V}{\partial y}\right)^2 + \left(\frac{\partial V}{\partial z}\right)^2\right]dV_k\,. \tag{18}$$

Where ε_k and V_k represent the permittivity and the volume of the k^{th} tetrahedron element, respectively. Thus, the total energy and losses in the entire composite can be written by summation over the n_k elements such as:

$$W_e = \sum_{k=1}^{n_k} W_e^k \tag{19}$$

$$P_e = \sum_{k=1}^{n_k} P_e^k \tag{20}$$

To compute quantities W_e and P_e, we suppose that the composite material is embedded in a plane capacitor. This way allows us to determine the effective permittivity in a direction parallel to the applied electric field. Then, from the capacitor electrostatic energy expression, we deduce the effective (complex) permittivity. We find that the real part, ε_{eff}', and imaginary one, ε_{eff}'', parallel to the applied electric field, are given by:

$$W_e^k = \frac{1}{2}\varepsilon_{eff}'\frac{S_d}{L_3}(V_2 - V_1)^2\,, \tag{21}$$

$$P_e^k = \frac{1}{2}\omega\varepsilon_{eff}''\frac{S_d}{L_3}(V_2 - V_1)^2\,. \tag{22}$$

Where V_1 and V_2 are the potentials applied across to plates of the unit cell (Fig. 2). Here, $S_d = L_1.L_3$ is the surface of in-depth. The real and imaginary parts of the effective permittivity then depends on the total energy, W_e, losses, P_e, linear size L_2 and applied potential difference $V_2 - V_1$. In addition, the second one is frequency-dependent. If the amplitude of the applied field is equal to 1, so the potential difference is kept equal to $\Delta V = L_2$. The following paragraph will be devoted to the determination of the optical properties of the material under investigation.

3-3 absorption-cross-section

From the evolution of the effective complex dielectric function depending on the wavelength (or frequency) of the incident field, the resonance modes that may occur in nanoparticles are identified. For this, it would be interesting to calculate the scattering cross-sections and absorption. The sum of these two quantities defines the extinction cross-section

$$\sigma_{ext} = \sigma_{abs} + \sigma_{diff}\,. \tag{23}$$

In the case where the dimensions are very small compared to the wavelength, the light scattering can be ignored, and we have: $\sigma_{ext} \approx \sigma_{abs}$

The cross-section of extinction *(absorption)* can be determined from the imaginary part of the effective dielectric function of the composite using the following equation [89]

$$\sigma_{abs} = \frac{V_p}{f}\frac{k}{n_{eff}}\varepsilon_{eff}''\,. \tag{24}$$

Here, V_p stands for the common volume of nanoparticles, f is their fraction, k is the wave-vector amplitude of the electromagnetic wave, and n_{eff} represents the refractive index that can be related to the real and imaginary parts, ε_{eff}' and ε_{eff}'', of the effective permittivity by (e.g. [90])

$$n_{eff} = \left(\frac{\sqrt{\varepsilon_{eff}''^2 + \varepsilon_{eff}''^2} + \varepsilon_{eff}'}{2}\right)^{1/2}\,. \tag{25}$$

This formula clearly shows that the peak of $\mathrm{Im}(\varepsilon_{eff})$ indicates that the light is rather absorbed in specific regions. The effective dielectric function and the effective refraction index are calculated using FEM. Hence, the section of optical absorption is easily obtained. In the following section, we present and discuss our findings.

IV. RESULTS AND DISCUTION

In this work we are interested in the study of the optical properties of two coupled gold nanoparticles coated with polymer shell using the FEM. For this nanocomposite system the variation of the conformation of polymers chains can lead to the formation of aggregates of nanoparticles. In particular the conformation of polymer chain depends on several environmental stimuli such as the temperature, PH, Solvents, Electromagnetic radiation (UV, visible) and others. The Fig.3 shows a schematic illustration of the assembly mechanism of the gold nanoparticles by the stimuli-responsive polymers intermediaries grafted on their surfaces. The stimuli collapse of polymer chains onto solid cores will decrease the spatial occupy and the surface property when the distance between two nanoparticles becomes very small the coupling effect exchange the interaction process of these nanoparticles with an incident electromagnetic wave which modifies the SPR properties of these nanoparticles.

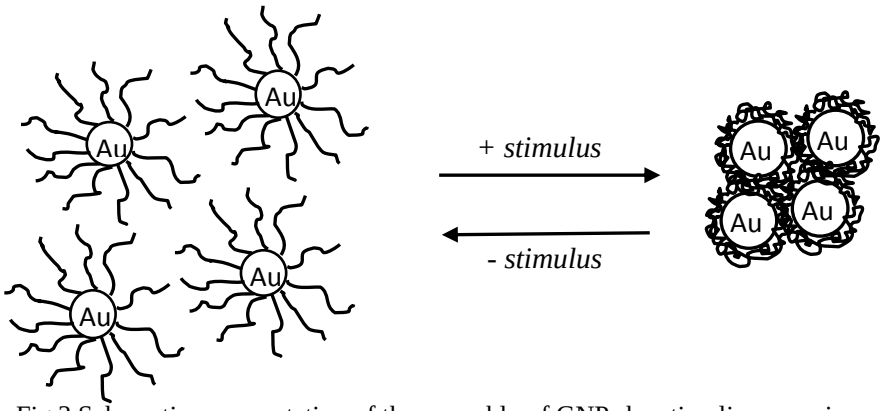

Fig.3 Schematic representation of the assembly of GNPs by stimuli-responsive polymers

To respect the limits imposed by the quasi-static approximation used in this simulation we are limiting our study in the case of binary coupling coated GNPs. For this, we consider two coupled GNPs with different configurations as shown in Fig.4, for these nanostructures the dependence of SPR on the shell thickness, permittivity of the polymer shell and gold-core radius will be discussed systematically.

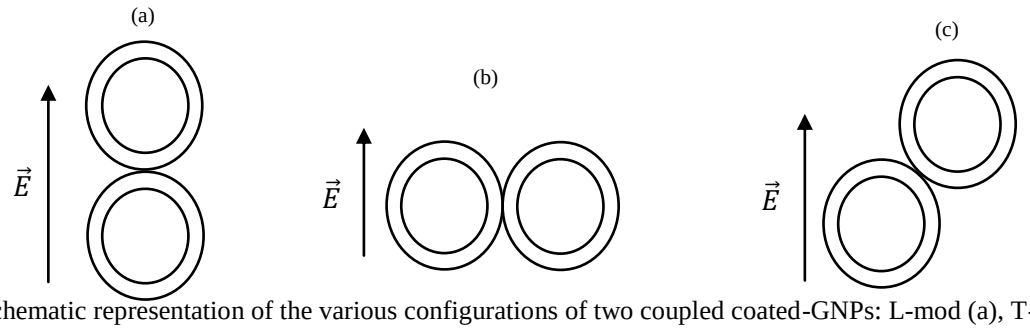

Fig.4 Schematic representation of the various configurations of two coupled coated-GNPs: L-mod (a), T-mode (b) and randomly oriented (c)

Let us consider two gold nanoparticles coated with a polymeric shell into contact and are emerged in aqueous dielectric medium, these nanoparticles are disposed such that the interparticles axis is parallel to the direction of external applied electric field called longitudinal mode (L-mode). The shell thickness of the polymer depends on several parameters such as the degree of polymerization, the quality of solvent and other external stimulated. When the thickness of polymeric shell decreases, the gold cores becomes closer the one to other. This closer induces a change in the plasmonic properties of these nanoparticles. In Fig.5 we represent the variation of the absorption cross-section versus the photon energy of two coated GNPs coupled to L-mode for different values of the thickness of the polymer-shell, for this figure: the radius of gold-core is set to ($R_c = 15nm$), the volume fraction of inclusions which is the ratio of the total volume of inclusions on the volume of the cell ($f = 0.1$) and permittivity of different phases of system are chosen as follows: dielectric medium ($\varepsilon_m = 1.77$), polymer-shell ($\varepsilon_p = 3.5$) and the permittivity of the gold-core is described by the two-CPDM These curves show that for the large values of polymer-shell thickness the SPR-peak position (λ_{max} -position) remains unchanged, in this case the polymer-shells has an effect shielded the coupling of gold-cores while for small values of the polymer-shell thickness the λ_{max} -position is red shift , in this case the coupling effect becomes very important compared to shielding effect.

In Fig.6 we represent the absorption cross-sections in the case where the two coated-GNPs are aligned perpendicular to the direction of the external applied field called transverse mode (T-mode), These curves show that when the thickness of polymer-shell decreases, the λ_{max} -position moves slightly to larger values of the photon energy that is to say blue-shift while the amplitude of the peak decreases. These results are in agreement with those found by W. Rechberger *et al* (e.g. [91]) in the case of GNPs without shells, the same results are also found by benhamou *et al* (e.g. [92]) in the case of an isolated coated-GNP. These results are explained by the absence of coupling between the two coated-GNPs in the case where the interparticles axis is perpendicular to the direction of external applied field.

Generally two nanoparticles which are located near one to other are randomly aligned relative to the direction of the external electric field, in order to model this configuration we presented in Fig.7 the results of the FEM simulation for two coupled coated-GNPs in the case where the angle between the interparticles axis and the field direction is ($\alpha = \pi/4$). For this figure we have chosen the following parameter values: radius of gold-core $R_c = 15nm$, volume fraction of inclusions $f = 0.1$, permittivity of surrounding medium $\varepsilon_m = 1.77$ and permittivity of polymer-shell $\varepsilon_p = 3.5$. These curves show that when the thickness of polymer-shell varied from $e = 4nm$ to $e = 10nm$ the λ_{max} -position remains unchanged and its amplitude undergoes a remarkable decrease while for the values much lower than $e = 4nm$ the λ_{max} -position is red-shift and it is noted the appearance of a second less intensive peak in the blue region the latter is due to particle-particle interaction (quadrupole interaction).

We note that these results are in agreement with the experimental results obtained by C. Durand-Gasselin *et al* (e.g. [93], [94]).These authors are interested in their work by the synthesis of assembled gold nanoparticles by thermosensitive polymers grafted on their surfaces. Specifically, they studied the synthesis and the preparation of GNPs suspensions stabilized by thermosensitive polymers that are the poly *(ethylene oxide-st-propylene oxide)*, ($EO_x - st - PO_y$) functionalized dithiol grouping in aqueous solution and also studied their behavior in solution. At low temperatures, all GNPs suspensions stabilized by the thermosensitive polymers exhibit a UV-visible absorption spectrum characteristic of GNPs when they are well-dispersed with a band of SPR characteristic centered at 520nm. When the temperature increases, the thermosensitive polymer chains grafted undergoing a phase transition, that is to say, they tend to dehydrate and become hydrophobic. Thereafter, from a critical temperature called T_{agg}, an aggregation of GNPs, characterized by a shift in the SPR-peak position to longer wavelengths is observed. These authors have shown also that the aggregation process is completely reversible that is the maximum of the SPR-peak position returns to its initial value when the temperature decreases below T_{agg}

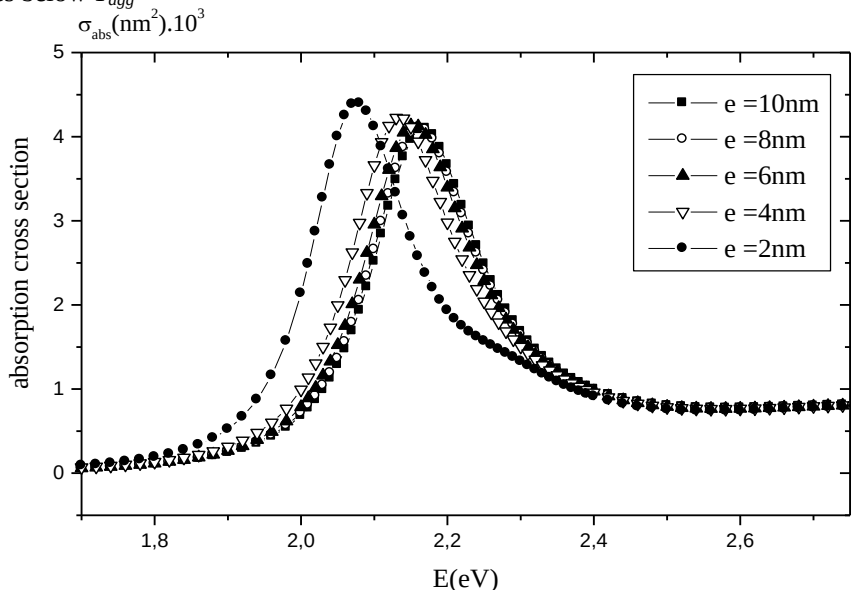

Fig.5 Absorption cross-section for L-mode of tow coated-GNPs for different values of the shell-thickness e. The curves are drawn choosing $f = 0.1$, $\varepsilon_m = 1.77$, $\varepsilon_p = 3.5$ and $R_c = 15nm$

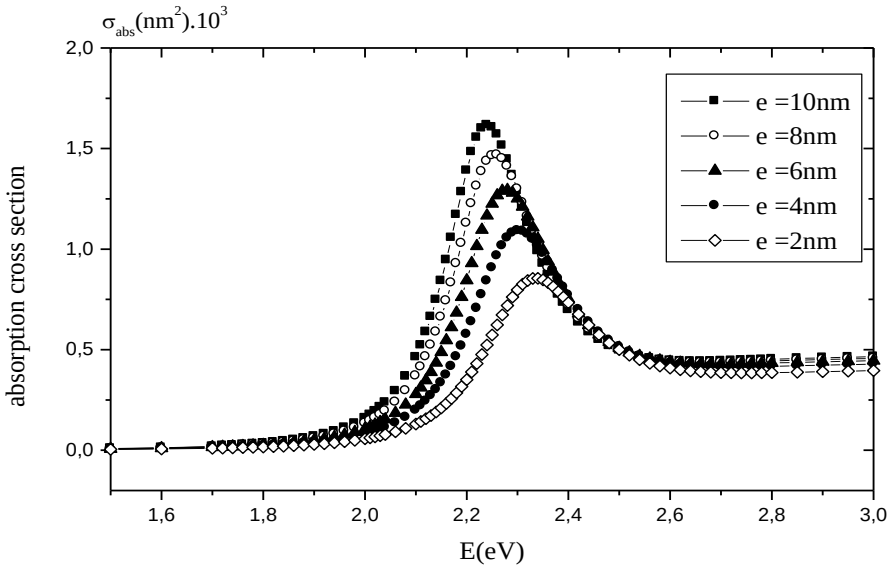

Fig.6 Absorption cross-section for T-mode of tow coated-GNPs for different values of the shell-thickness e. The curves are drawn choosing $f = 0.1$, $\varepsilon_m = 1.77$, $\varepsilon_p = 3.5$ and $R_c = 15nm$

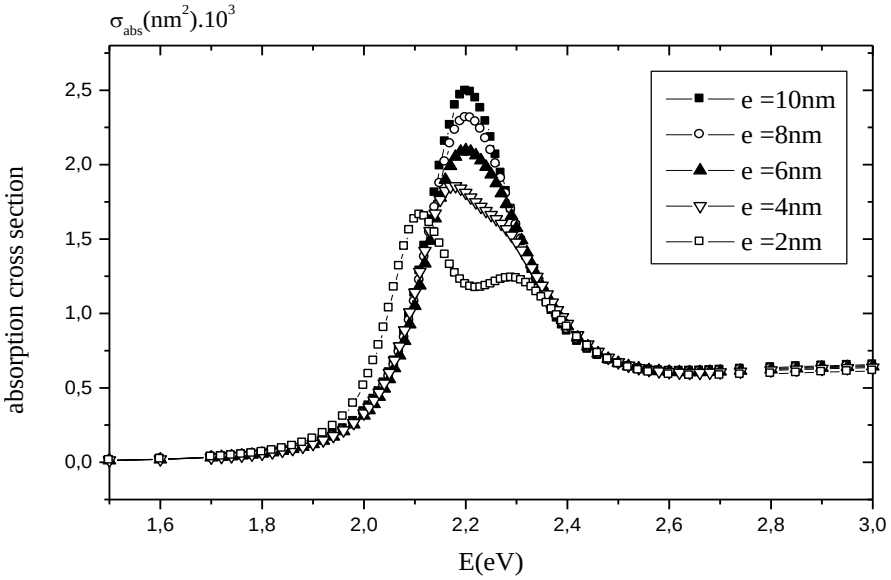

Fig. 7 Absorption cross-section for the random disposition of tow coated-GNPs for different values of the shell-thickness e. The curves are drawn choosing $f = 0.1$, $\varepsilon_m = 1.77$, $\varepsilon_p = 3.5$ and $R_c = 15nm$

In the following step we will study the effect of polymer-shell permittivity on the optical properties of two coupled coated-GNPs. Indeed, the permittivity of polymer layer coating metal nanoparticle depends on several parameters, for example the grafting density, solvent quality and the polymers nature. Fig.8 shows the variation of the absorption cross-section of two coated GNPs coupled into L-mode for different values of polymer-shell permittivity, for this figure we have fixed the value of shell thickness to $e = 4nm$ and the other parameters $f = 0.1$, $R_c = 15nm$ and $\varepsilon_m = 1.77$. These curves show that when the polymer-shell permittivity increases from $\varepsilon_p = 3$ to $\varepsilon_p = 5$, the absorption amplitude increases considerably while the SPR peak position moves from ($E = 2.17eV, \lambda_{max} = 572nm$) to ($E = 2.04eV, \lambda_{max} = 608nm$) this means that the λ_{max} -position is red-shift, these results show that the coupling effect becomes important when the polymer-shell permittivity increases for the L-mode coupling. The simulation results of the effect of polymer-shell permittivity for the T-mode are shown in Fig.9, these curves shows that when the polymer-shell permittivity increases the SPR peak position is slightly red-shift ($\lambda_{max} = 535nm$ for $\varepsilon_p = 3$ and $\lambda_{max} = 551nm$ for $\varepsilon_p = 5$) and the amplitude of the peak is also increases. These results are also remarked by benhamou *et al* [92] for insulated coated-GNP, these results are interpreted by the absence of the coupling effect for the T-mode configuration

Fig.10 shows the variation of the absorption cross-section for deferent values of polymer-shell permittivity in the case where the interparticles axis is randomly oriented relative to the external field. This figure shows that when the permittivity ε_s varies from $\varepsilon_p = 3$ to $\varepsilon_p = 5$, the λ_{max} -position is red-shift from ($E = 2.22eV, \lambda_{max} = 559nm$) to ($E = 2.08eV, \lambda_{max} = 596nm$)and the amplitude increases, these curves also show that from $\varepsilon_p = 4.5$ begins to appear a second peak around the $\lambda_{max} = 564nm$ which is due to the quadripolar interaction. These results show clearly that the coupling effect becomes significant when the polymer-shell permittivity increases.

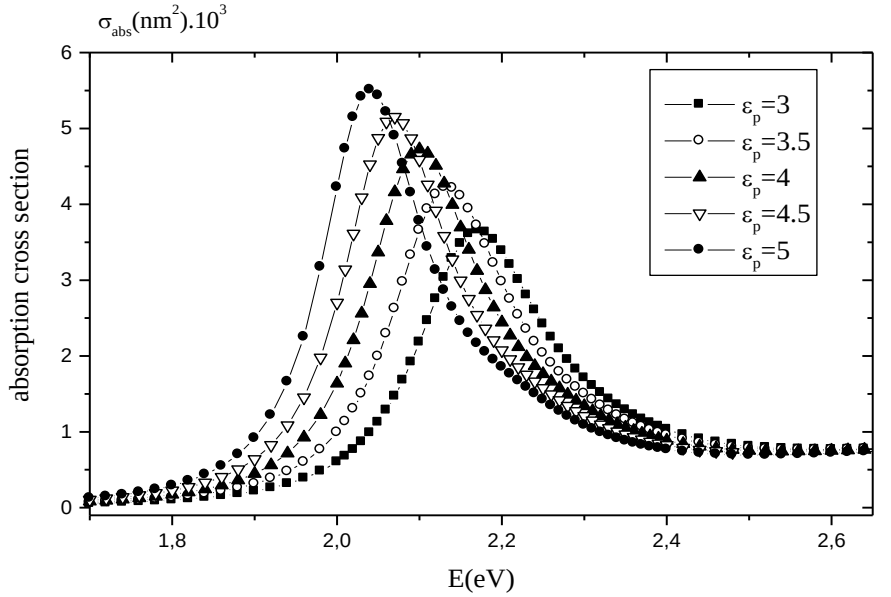

Fig. 8 Absorption cross-section for L-mode of tow coated-GNPs for different values of the shell-thickness permittivityε_p. The curves are drawn choosing $f = 0.1$, $\varepsilon_m = 1.77$, $e = 4nm$ and $R_c = 3.5nm$

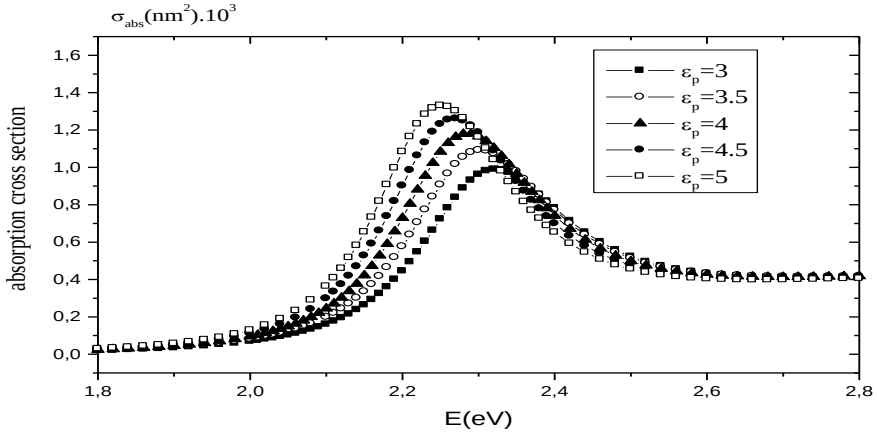

Fig.9 Absorption cross-section for T-mode of tow coated-GNPs for different values of the shell-thickness permittivityε_p. The curves are drawn choosing $f = 0.1$, $\varepsilon_m = 1.77$, $e = 4nm$ and $R_c = 3.5nm$

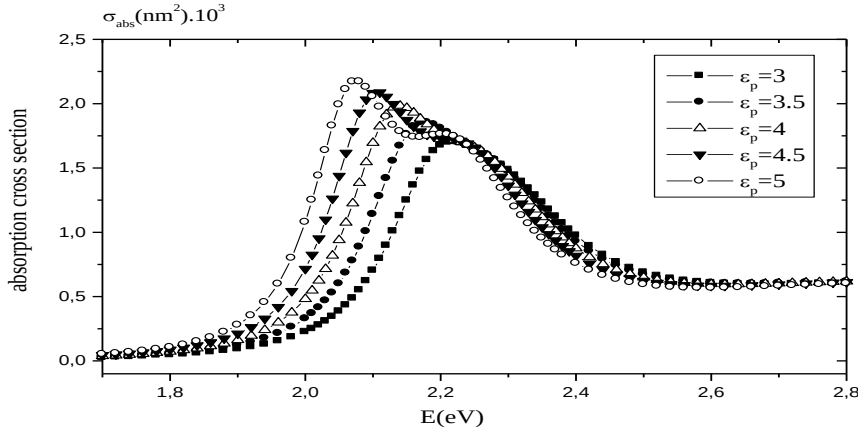

Fig.10 Absorption cross-section for the random disposition of tow coated-GNPs for different values of the shell-thickness permittivityε_p. The curves are drawn choosing $f = 0.1$, $\varepsilon_m = 1.77$, $e = 4nm$ and $R_c = 3.5nm$

Now consider two gold-core/polymer-shell nanoparticles placed in contact and emerged in a dielectric medium of permittivity $\varepsilon_m = 1.77$. For these nanocomposites the two parameters: thickness and permittivity of the external polymer layer may simultaneously vary following an external stimulated response which can be either physical, such as temperature in the case of thermosensitive polymers, PH or Electromagnetic radiation (UV, visible), chemical as Specific ions and Chemical agents or biological as Enzyme substrates and Affinity ligands. In Figs.11-13 we present the simulation results obtained by the FEM for deferent configurations: L-mode T-mode and randomly oriented, for these figures the variation of the thickness and permittivity of the polymer-shell is simultaneously: the first decreases the same time as the second increases. These curves show that the λ_{max} -position of SPR is red-shift when the shell-thickness decreases and the polymer-shell permittivity increases in the case of L-mode and in the case where the two coupled coated-GNPs are randomly oriented relative to the external field whereas for the T-mode SPR λ_{max} -position is slightly varied. The main conclusion is that the coupling effect becomes significant when the polymer-shell thickness decreases and its permittivity increases in the case where the two coupled nanoparticles are randomly or longitudinally disposed relative to the direction of the applied electric field.

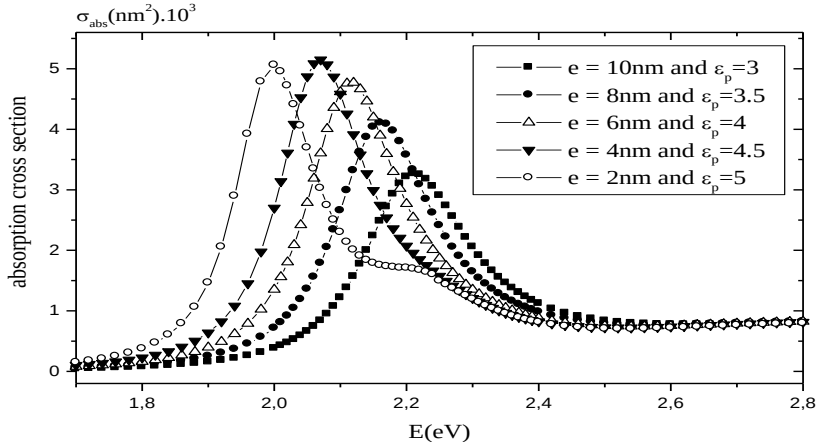

Fig.11 Absorption cross-section for the L-mode of tow coated-GNPs for different values of the shell-thickness permittivityε_p.and shell-thickness e.The curves are drawn choosing $f = 0.1$, $\varepsilon_m = 1.77$ and $R_c = 15nm$

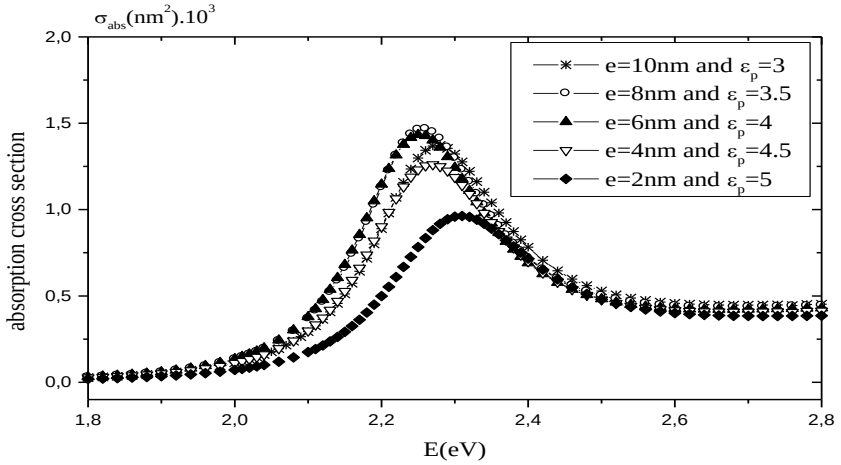

Fig.12 Absorption cross-section for the T-mode of tow coated-GNPs for different values of the shell-thickness permittivity ε_p.and shell-thickness e.The curves are drawn choosing $f = 0.1$, $\varepsilon_m = 1.77$ and $R_c = 15nm$

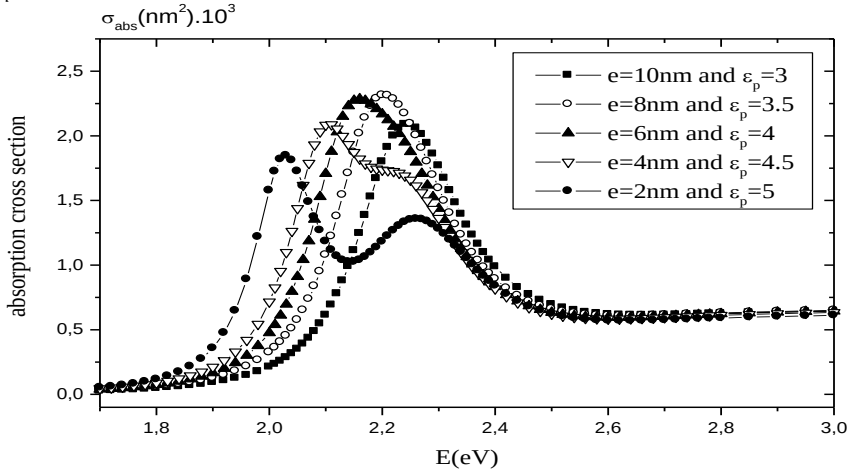

Fig.13 Absorption cross-section for the random disposition of tow coated-GNPs for different values of the shell-thickness permittivity ε_p.and shell-thickness e.The curves are drawn choosing $f = 0.1$, $\varepsilon_m = 1.77$ and $R_c = 15nm$

Finally we studied the effect of gold-core radius on the optical properties of two coupled coated-GNPs, for this we have chosen the following parameters: f = 0.1, $\varepsilon_m = 1.77$, $\varepsilon_p = 3.5$ and e = 4nm. Fig.14 shows the variation of the absorption cross-section for different values of core-radius for the L-mode configuration, these curves show that when the core-radius takes the values $R_c = 10$nm, $R_c = 15$nm and $R_c = 20$nm the SPR peak occurred for the wavelength respectively while the peak amplitude of the SPR increases considerably $\lambda_{max} = 577$nm, $\lambda_{max} = 582$nm and $\lambda_{max} = 588$nm while the absorption intensity increases considerably. Fig.15 shows a small shift of the SPR peak position in the case of T-mode configuration while the amplitude is much more pronounced when the gold core-radius increases. In the case where the two nanoparticles are randomly arranged Fig.16 shows that when the gold core-radius increases, the position of the SPR is red-shift and increases in amplitude and we also note the appearance of a shoulder of the peak near the blue wavelengths which mean that the coupling effect becomes very important when the gold core-radius increases.

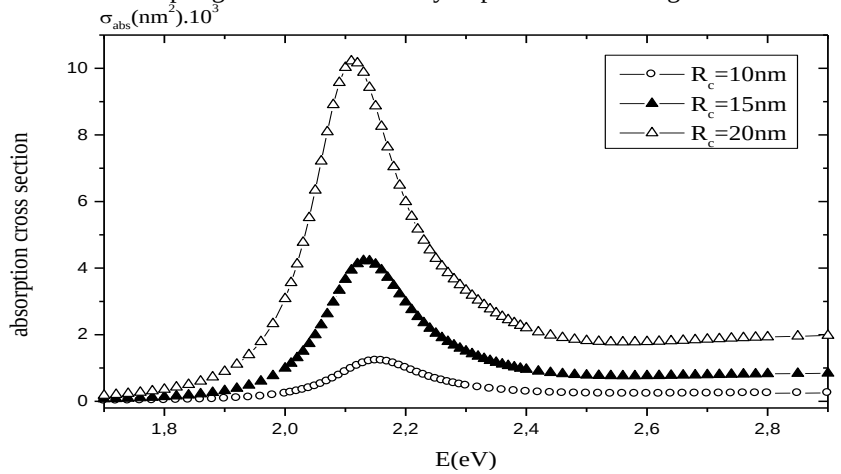

Fig.14 Absorption cross-section for the L-mode of tow coated-GNPs for three values of the gold-core radius R_c.The curves are drawn choosing $f = 0.1$, $\varepsilon_m = 1.77$, $e = 4nm$ and $\varepsilon_p = 3.5$

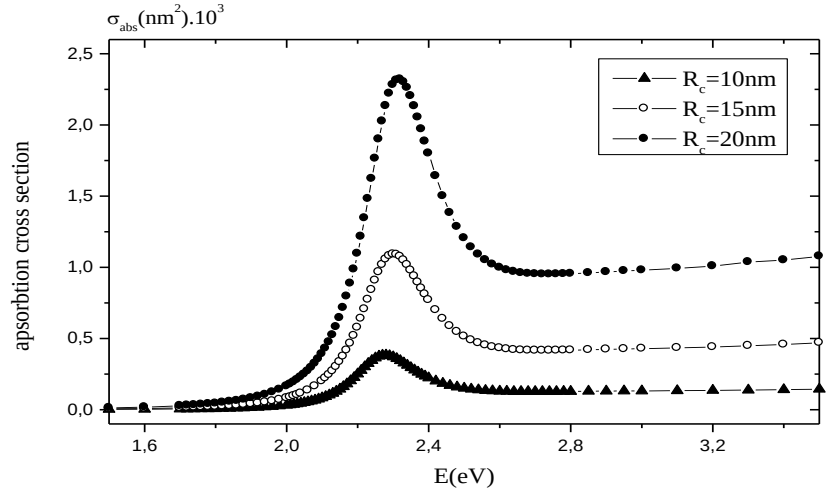

Fig.15 Absorption cross-section for the T-mode of tow coated-GNPs for three values of the gold-core radius R_c .The curves are drawn choosing $f = 0.1$, $\varepsilon_m = 1.77$, $e = 4nm$ and $\varepsilon_p = 3.5$

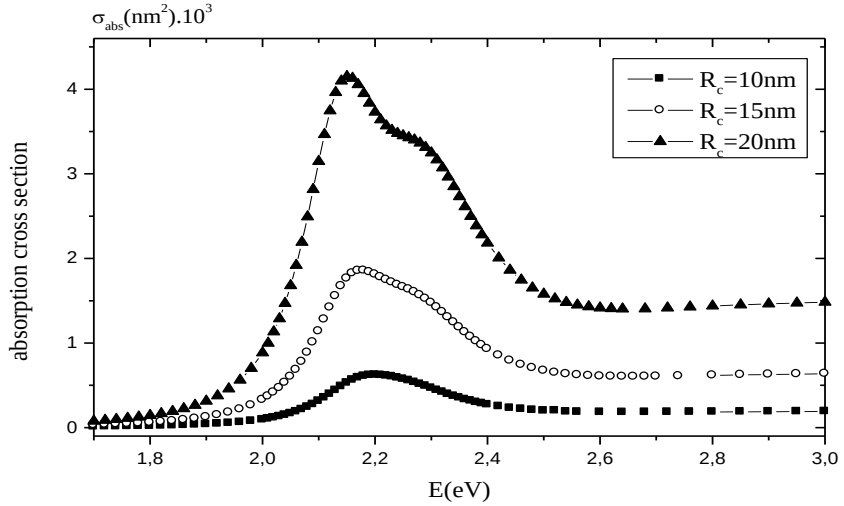

Fig.16 Absorption cross-section for the random disposition of tow coated-GNPs for three values of the gold-core radius R_c .The curves are drawn choosing $f = 0.1$, $\varepsilon_m = 1.77$, $e = 4nm$ and $\varepsilon_p = 3.5$

V. CONCLUDING REMARKS

We recall that the aim of this work was to study the optical properties of GNPs coupled through stimuli-responsive polymers shells, for this we have established a series of 3D-simulations using FEM to calculating the absorption cross-section of two coated-GNPs with different configurations called modes: the longitudinal mode (L-mode) where the tow GNPs are arranged parallel to the direction of the applied electric field, the transverse mode (T-mode) where the two GNPs are arranged perpendicular to the field direction and the random mode where the tow GNPs are disposed randomly relative to the field direction. For these modes we studied the effect of geometrical and physical parameters on the plasmonic properties of two assembled coated-GNPS such as the permittivity and thickness of the polymer-shell and the gold-core radius.

In the case of L-mode, the results show that for the great values of the shell-thickness, the position and amplitude of SPR peak does not change but when it became less than a given threshold the λ_{max}-position is red-shift and the amplitude increases slightly. For this same mode we note that when the shell-permittivity increases, the SPR-peak moves strongly to the wavelengths near the red and its amplitude also increases, whereas when the gold-core radius increases the λ_{max}-position is slightly red-shift and the peak amplitude is strongly increases. The essential conclusions from these results is that when the $\frac{e}{R_c}$ ratio decreases, the SPR-peak position is red-shifts whereas the amplitude increases when e and *(or)* R_c increases

In the case of T- mode the obtained results show that the coupling effect between the two GNPS does not depend on the parameters e , ε_p and R_c , for this mode the obtained absorption spectres have the same behaviour as in the case of the isolated coated-GNP

The latest configuration that we have studied is the case where the two GNPs are randomly oriented relative to the direction of applied electric field. For this configuration the obtained results showed that the coupling effect depends on the parameters e , ε_p and R_c , the absorption spectra show that, when the polymer-shell thickness decreases, the polymer-shell permittivity increases or the gold-core radius increases, the λ_{max}-position is red-shift and we notice the appearance of a second peak due to the particle-particle interaction.

Finally, we emphasize that the numerical method developed in this work, for the investigation of the optical properties of the assembled coated GNPs, can be extended to other types of Gold nanoparticles, such as noble metallic nanoalloys of different shapes and morphology in order to improve the optical properties suitable for the biomedical applications. In addition, we emphasize that the numerical method, developed in this paper, can be extended to investigate the electromagnetic coupling between particles and its effect on the plasmonic behaviors. Such considerations are in progress.

ACKNOWLEDGMENT

All of authors would like to thank Pr. M. Benhamou, member of the Polymer Physics and Critical Phenomena Laboratory, Sciences Faculty Ben M'sik,, Casablanca , Morocco, actually, Professor at the, ENSAM, Moulay Ismail University, Meknes, Morocco, for helpful discussions.

(A.D) and (F.B) would like to thank the TlemcenUniversiyt of Algeria, for their kind hospitality during their regular visits.

REFERENCES

[1] J. Yguerabide and E.E. Yguerabide, "Light-scattering submicroscopic particles as highly fluorescent analogs and their use as tracer labels in clinical and biological applications," *Analytical Biochemistry*, vol. 262, pp. 137–156, 1998.

[2] J. Yguerabide and E.E. Yguerabide, "Light-scattering submicroscopic particles as highly fluorescent analogs and their use as tracer labels in clinical and biological applications: Experimental characterization," *Analytical Biochemistry*, vol. 262, pp. 157–176, 1998.

[3] K.L. Kelly, E. Coronado, L.L. Zhao and G.C. Schatz, "The optical properties of metal nanoparticles: the influence of size, shape, and dielectric environment," *The Journal of Physical Chemistry. B*, vol. 107, pp. 668–677, 2003.

[4] V. Degiorgio and R. Piazza, "Light scattering in colloid and interface science," *Current Opinion in Colloid and Interface Science*, vol. 1, pp. 11–16, 1996.

[5] R. Sardar, A.M. Funston, P. Mulvaney and R.W. Murray, "Gold nanoparticles: past, present, and future," *Langmuir*, vol. 25, pp. 13840–13851, 2009.

[6] K. Kneipp, H. Kneipp, I. Itzkan, R.R. Dasari and M.S. Feld, "Ultrasensitive chemical analysis by Raman spectroscopy," *Chemical Reviews*, vol. 99, pp. 2957–2976, 1999.

[7] I. Delfino, A.R. Bizzarri and S. Cannistraro, "Single-molecule detection of yeast cytochrome by surface-enhanced Raman spectroscopy," *Biophysical Chemistry*, vol. 113, pp. 41–51, 2005.

[8] I. Delfino, A.R. Bizzarri and S. Cannistraro, "Time-dependent study of single-molecule SERS signal from yeast cytochrome c," *Chemical Physics*, vol. 326, pp. 356–362, 2006.

[9] S.E. Lohse and C.J. Murphy, "Applications of colloidal inorganic nanoparticles: from medicine to energy," *Journal of the American Chemical Society*, vol. 134, pp. 15607–15620, 2012.

[10] K. Saha, S.S. Agasti, C. Kim, X. Li and V.M. Rotello, "Gold nanoparticles in chemical and biological sensing," *Chemical Reviews*, vol. 112, pp. 2739–2779, 2012.

[11] A. Liang, Q. Liu, G. Wen and Z. Jiang, "The surface-plasmon-resonance effect of nanogold/silver and its analytical applications," *TRAC Trends in Analytical Chemistry*, vol. 37, pp. 32–47, 2012.

[12] P.K. Jain, K.S. Lee, I.H. El-Sayed and M.A. El-Sayed, "Calculated absorption and scattering properties of gold nanoparticles of different size, shape, and composition: applications in biological imaging and biomedicine," *The Journal of Physical Chemistry.B*, vol. 110, pp. 7238–7248, 2006.

[13] C.F. Bohren and D.R. Huffman, *Absorption and Scattering of Light by Small Particles*, John Wiley & Sons, Inc., New York, 1983.

[14] Papavassiliou and G. C. Prog, "optical properties of small inorganic and organic metal particles," *Solid State Chem*., vol. 12, pp. 158-271, 1980.

[15] P. K. Aravind, A. Nitzan and H. Metiu, "The interaction between electromagnetic resonances and its role in spectroscopic studies of molecules absorbed on colloidal particles or metal spheres," *H. Surf. Sci*., vol. 110, pp. 189-204, 1981.

[16] M. Quinten and U. Kreibig, "Absorption and elastic scattering of light by particle aggregates," *U. Appl. Opt.*,vol. 32, pp. 6173-6182, 1993.

[17] U.Kreibig, A.Althoff and H.Pressmann, "Veiling of optical single particle properties in many particle systems by effective medium and clustering effects," Surf. Sci., vol. 106, pp. 308-317, 1991.

[18] M. Quinten and U. Kreibig, "Optical properties of aggregates of small metal particles," *U. Surf. Sci*., vol. 172, pp. 557-557, 1986.

[19] A. N. Shipway, M. Lahav, R. Gabai,and I. Willner, "Investigation into the Electrostatically-Induced Aggregation of Au-Nanoparticles," *Langmuir*, vol. 16, pp. 8789-8795, 2000.

[20] P. Dimon, S. K.Sinha, D. A. Weitz, C. R. Safinya, G. S. Smith, W. A. Varady and H. M. Lindsay, "structure of aggregated gold colloids," *Phys. ReV. Lett*., vol. 57, pp. 595-598, 1986.

[21] W.Y. Shih, J. Liu, W. H. Shih and I.A. Aksay, "Aggregation of Colloidal Particles with a Finite Interparticle Attraction Energy," *J. Stat. Phys.*, vol. 62, pp. 961-984, 1991.

[22] K. S. Mayya, V. Patil, M. Sastry, "An optical absorption investigation of cross-linking of gold colloidal particles with dithol molecule," *Bull. Chem. Soc. Jpn*., vol. 73, pp. 1757-1761, 2000.

[23] C. G. Blatchford, J. R. Campbell and J. A. Creighton, "Plasma resonance-enhanced Raman scatteringby absorbates on gold colloids: the effects of aggregation," *Surf. Sci*., vol., 120,pp. 435-455, 1982.

[24] J. P. Wilcoxon, J. E. Martin and D. W. Schaefer, "Aggregation in colloidalgold," *Phys. ReV. A*, vol. 39, pp. 2675-2688, 1989.

[25] M. Brust, M. Walker, D. Bethell, D. J. Schiffrin, and R. Whyman, "Synthesis of thiol derivatized gold nanoparticles in a 2-phase liquid-liquid system," *J. Chem. Soc. Chem. Commun*, vol. 7, 801–802, 1994.

[26] J. M. de la Fuente, A. G. Barrientos, T. C. Rojas, J. Rojo, J. Canada, A. Fernandez, and S. Penades, "Gold glyconanoparticles as water-soluble polyvalent models to study carbohydrate interactions," *Angewandte Chemie-international Edition*, vol. 40(12), pp. 2258 +-, 2001.

[27] J. J. Storhoff, A. A. Lazarides, R. C. Mucic, C. A. Mirkin, R. L. Letsinger, and G. C. Schatz. "What controls the optical properties of dna-linked gold nanoparticle assemblies," *Journal of the American Chemical Society*, vol. 122(19), pp. 4640–4650, May 2000.

[28] Y. W. Cao, R. Jin, and C. A. Mirkin, "DNA-modified core-shell ag/au nanoparticles," *Journal of the American Chemical Society*, vol. 123(32), pp. 7961–7962, Aug. 2001.

[29] Z. Li, R. C. Jin, C. A. Mirkin, and R. L. Letsinger. "Multiple thiol-anchor capped dna gold nanoparticle conjugates," *Nucleic Acids Research*, vol. 30(7), pp. 1558–1562, April 2002.

[30] S. Bidault, F. J. G. de Abajo, and A. Polman , "Plasmon-based nanolenses assembled on a well-defined DNA template," *Journal of the American Chemical Society*, vol. 130(9), pp. 2750–+, March 2008.

[31] J. Y. Kim and J. S. Lee, "Synthesis and thermally reversible assembly of DNA-gold nanoparticle cluster conjugates," *Nano. Lett.*, vol. 9(12), pp.4564–4569, December 2009.

[32] I. Y. Galaev and B. Mattiasson, "'smart' polymers and what they could do in biotechnology and medicine," *Trends In Biotechnology*, vol. 17(8), pp. 335–340, August 1999.

[33] Y. J. Kang and T. A. Taton, "Core/shell gold nanoparticles by self-assembly and crosslinking of micellar, block-copolymer shells," *Angewandte Chemie-international Edition*, vol. 44(3), pp. 409–412, 2005.

[34] M. Karg, I. Pastoriza-Santos, L. M. Liz-Marzan, and T. Hellweg, "A versatile approach for the preparation of thermosensitive pnipam core-shell microgels with nanoparticle cores," *Chem. Phys. Chem*., vol. 7(11), pp. 2298–2301, November 2006.

[35] J. D. Gibson, B. P. Khanal, and E. R. Zubarev, "Paclitaxel-functionalized gold nanoparticles," *Journal of the American Chemical Society*, vol. 129(37), pp. 11653–11661, September, 2007.

[36] P. Ghosh, G. Han, M. De, C. K. Kim, and V. M. Rotello, "Gold nanoparticles in delivery applications," *Advanced Drug Delivery Reviews*, vol. 60(11), pp. 1307–1315, August 2008.

[37] Y. Y. Yuan, X. Q. Liu, Y. C. Wang, and J. Wang, "Gold nanoparticles stabilized by thermosensitive diblock copolymers of poly(ethylene glycol) and polyphosphoester," *Langmuir*, vol. 25(17), pp.10298–10304, September 2009.

[38] Deo T. Miles W. PeterWuelfing, Stephen M. Gross and Royce W. Murray, "Nanometer gold clusters protected by surface-bound monolayers of thiolated poly(ethylene glycol) polymer electrolyte," *J. Am. Chem. Soc*., vol. 120, pp. 12696–12697, 1998.

[39] M. K. Corbierre, N. S. Cameron, and R. B. Lennox"Polymer-stabilized gold nanoparticles with high grafting densities," *Langmuir*, vol. 20(7), pp. 2867–2873, March 2004.

[40] F. Seker, P. R. L. Malenfant, M. Larsen, A. Alizadeh, K. Conway, A. M. Kulkarni, G. Goddard, and R. Garaas" On-demand control of optoelectronic coupling in gold nanoparticle arrays," *Advanced Materials*, vol. 17(16), pp. 1941–+, August 2005.

[41] A. B. Lowe, B. S. Sumerlin, M. S. Donovan, and C. L. McCormick"Facile preparation of transition metal nanoparticles stabilized by well-defined (co)polymers synthesized via aqueous reversible addition-fragmentation chain transfer polymerization," *Journal of the American Chemical Society*, vol. 124(39), pp. 11562–11563, October 2002.

[42] C. Mangeney, F. Ferrage, I. Aujard, V. Marchi-Artzner, L. Jullien, O. Ouari, E. D. Rekai, A. Laschewsky, I. Vikholm, and J. W. Sadowski, "Synthesis and properties of water-soluble gold colloids covalently derivatized with neutral polymer monolayers," *Journal of the American Chemical Society*, vol. 124(20), pp. 5811–5821, May 2002.

[43] I. Hussain, S. Graham, Z. X. Wang, B. Tan, D. C. Sherrington, S. P. Rannard, A. I. Cooper, and M. Brust, "Size-controlled synthesis of near-monodisperse gold nanoparticles in the 1-4 nm range using polymeric stabilizers," *Journal of the American Chemical Society*, vol. 127(47), pp. 16398–16399, November 2005.

[44] C. Chevigny, D. Gigmes, D. Bertin, J. Jestin, and F. Boué, "Polystyrene grafting from silica nanoparticles via nitroxide-mediated polymerization (NMP): synthesis and SANS analysis with the contrast variation method," *Soft Matter*, vol. 5(19), pp. 3741–3753, 2009.

[45] J. Oberdisse, J. Jestin, G. Carrot, A. El Harrak and F. Boue, "Polymer grafting from 10-nm individual particles: proving control by neutron scattering," *Soft Matter*, vol. 2, pp. 1043–1047, 2006.

[46] K. Ohno, K. Koh, Y. Tsujii, and T. Fukuda, "Synthesis of gold nanoparticles coated with well-defined, high-density polymer brushes by surface-initiated living radical polymerization," *Macromolecules*, vol. 35(24), pp. 8989–8993, November 2002.

[47] H. Y. Zhao, X. L. Kang, and L. Liu, "Comb-coil polymer brushes on the surface of silica nanoparticles," *Macromolecules*, vol. 38(26), pp. 10619–10622, December 2005.

[48] A. B. Lowe and C. L. McCormick, "Reversible addition-fragmentation chain transfer (raft) radical polymerization and the synthesis of water-soluble (co)polymers under homogeneous conditions in organic and aqueous media," *Progress In Polymer Science*, vol. 32(3), pp. 283–351, March 2007.

[49] J. Chiefari, Y. K. Chong, F. Ercole, J. Krstina, J. Jeffery, T. P. T. Le, R. T. A. Mayadunne, G. F. Meijs, C. L. Moad, G. Moad, E. Rizzardo, and S. H. Thang, "Living free-radical polymerization by reversible addition-fragmentation chain transfer: The raft process," *Macromolecules*, vol. 31(16), pp. 5559–5562, 1998.

[50] G. Moad, J. Chiefari, Y. K. Chong, J. Krstina, R. T. A. Mayadunne, A. Postma, E. Rizzardo, and S. H. Thang, "Living free radical polymerization with reversible addition fragmentation chain transfer (the life of raft)," *Polymer International*, vol. 49(9), pp. 993–1001, September 2000.

[51] S. Perrier, P. Takolpuckdee, and C. A. Mars, "Reversible addition-fragmentation chain transfer polymerization: End group modification for functionalized polymers and chain transfer agent recovery," *Macromolecules*, vol. 38(6), pp. 2033–2036, March 2005.

[52] F. Ganachaud, M. J. Monteiro, R. G. Gilbert, M. A. Dourges, S. H. Thang, and E. Rizzardo, "Molecular weight characterization of poly(n-isopropylacrylamide) prepared by living free-radical polymerization," *Macromolecules*, 33(18), pp. 6738–6745, 2000.

[53] J. Shan, M. Nuopponen, H. Jiang, T. Viitala, E. Kauppinen, K. Kontturi, and H. Tenhu, "Amphiphilic gold nanoparticles grafted with poly(n-isopropylacrylamide) and polystyrene," *Macromolecules*, vol. 38(7), pp. 2918–2926, 2005.

[54] M. Nuopponen, J. Ojala, and H. Tenhu, "Aggregation behaviour of well defined amphiphilic diblock copolymers with poly (n-isopropylacrylamide) and hydrophobic blocks," *Polymer*, vol. 45(11), pp. 3643–3650, 2004.

[55] B. S. Lokitz, Y. Li and C. L. McCormick, "Raft synthesis of a thermally responsive abc triblock copolymer incorporating n-acryloxysuccinimide for facile in situ formation of shell cross-linked micelles in aqueous media," *Macromolecules*, vol. 39pp. 81–89, 2006.

[56] Y. K. Chong, T. P. T. Le, G. Moad, E. Rizzardo, and S. H. Thang, "A more versatile route to block copolymers and other polymers of complex architecture by living radical polymerization: The raft process," *Macromolecules*, vol. 32(6), pp. 2071–2074, March 1999.

[57] M. Q. Zhu, L. Q. Wang, G. J. Exarhos, and A. D. Q. Li, "Thermosensitive gold nanoparticles," *Journal of the American Chemical Society*, vol. 126(9), pp. 2656–2657, March 2004.

[58] J. R. Morones and W. Frey, "Environmentally sensitive silver nanoparticles of controlled size synthesized with pnipam as a nucleating and capping agent," *Langmuir*, vol. 23(15), pp. 8180-8186, July 2007.

[59] J. Shan and H. Tenhu, "Recent advances in polymer protected gold nanoparticles: synthesis, properties and applications," *Chemical Communications*, vol. (44), pp. 4580-4598, 2007.

[60] H. Zhang, J. S. Han, and B. Yang, "Structural fabrication and functional modulation of nanoparticle-polymer composites," *Adv. Funct. Mater*, vol. 20(10), pp. 1533-1550, 2010.

[61] O. J. Cayre, N. Chagneux, and S. Biggs, "Stimulus responsive core-shell nanoparticles: synthesis and applications of polymer based aqueous systems," *Soft Matter*, vol. 7(6), pp. 2211-2234, 2011.

[62] M. A. C. Stuart, W. T. S. Huck, J. Genzer, M. Mueller, C. Ober, M. Stamm, G. B. Sukhorukov, I. Szleifer, V. V. Tsukruk, M. Urban, F. Winnik, S. Zauscher, I. Luzinov, and S. Minko, "Emerging applications of stimuli-responsive polymer materials," *Nat. Mater*,.vol. 9(2), pp. 101-113, 2010.

[63] T. Chen, R. Ferris, J. Zhang, R. Ducker, and S. Zauscher, "Stimulus-responsive polymer brushes on surfaces: Transduction mechanisms and applications," *Prog. Polym. Sci.*, vol. 35(1-2), pp. 94-112, 2010.

[64] M. Motornov, Y. Roiter, I. Tokarev, and S. Minko, "Stimuli-responsive nanoparticles, nanogels and capsules for integrated multifunctional intelligent systems," *Prog. Polym. Sci.*, vol. 35(1-2), pp. 174-211, 2010.

[65] Gil ES and Hudson SA, "Stimuli-reponsive polymers and their bioconjugates," *Prog. Polym. Sci.*, vol. 29, pp. 1173–1222, 2004.

[66] Z. B. Hu, Y. Y. Chen, C. J.Wang, Y. D. Zheng, and Y. Li, "Polymer gels with engineered environmentally responsive surface patterns,".*Nature*, vol. 393, pp. 149–152, 1998.

[67] Y. Cui, C. Tao, S. P. Zheng, Q. He, S. F. Ai and J. B. Li, "Synthesis of thermosensitive PNIPAM-co-MBAA nanotubes by atom transfer radical polymerization within a porous membrane," *Macromol. Rapid Commun*, vol. 26, pp. 1552–1556, 2005.

[68] L. K. Ista, S. Mendez, V. H. Pérez-Luna and G. P. López, "Synthesis of Poly(N-isopropylacrylamide) on Initiator-Modified Self-Assembled Monolayers,". *Langmuir*, vol. 17, pp. 2552-2555, 2001.

[69] A. Fischer, A. Brembilla and P. Lochon, "Nitroxyde-Mediated Radical polymerization of 4-vinylpyridine: study of the pseudo-living character of the reaction and influence of Temperature and Nitroxyde concentration," *Macromolecules*, vol. 32, pp. 6069-6072, 1999.

[70] J. Bohrisch, U. Wendler and W. Jaeger, "Controlled radical polymerization of 4-vinylpyridine,"*Macromol Rapid Commun*, vol. 18, pp. 975-982, 1997.

[71] A. M. Mika and R. F. Childs, "Acid/base properties of poly(4-vinylpyridine) anchored within microporous membranes," *J Membr Sci.*, vol. 152, pp. 129-140, 1999.

[72] V. A. Baulin and A. Halperin, "Signatures of a Concentration-Dependent Flory χ Parameter: Swelling and Collapse of Coils and Brushes," *Macromol.Theory Simul*., vol. 12, pp. 549–559, 2003.

[73] V. A. Baulin, E. B. Zhulina and A. Halperin, "self-consistent field theory of brushes of neutral water-soluble polymers," *J Chem Phys*., vol. 119, pp. 10977-10988, 2003.

[74] R. H. Pelton, H. M. Pelton, A. Morphesis and R. L. Rowell, "Particle sizes and electrophoretic mobilities of poly(NIPAM) latex," *Langmuir*, vol. 5, pp. 816-818, 198.

[75] TJV. Prazeres, AA. Santos and JMG. Martinho, "Adsorption of oligonucleotides on PMMA/PNIPAM core-shell latexes: polarity of the PNIPAM shell probed by fluorescence," *Langmuir*, vol. 20, pp. 6834-6840, 2004.

[76] DJ. Gan and LA.Lyon, "Inerfacial nouraditive energy transfer in responsive core-shell hydrogel nanoparticles," *J Am Chem Soc.*, vol. 123, pp. 8203-8209, 2001.

[77] J.N. Reddy, *An Introduction to Finite Element Method*, 2nd., Mc Graw Hill, New York, 1993; See also O.C. Zienkiewicz and R.L. Taylor, *The Finite Element Method*, Vol. 1, McGraw-Hill, London, 1989.

[78] A.Akouibaa, M. Benhamou, A. Derouiche, "Simulation of the Optical Properties of Gold Nanorods : Comparison to Experiment", *IJARCSSE Journal*, vol. 3(9), 494, 2013.

[79] K.W YU, P. M. Hui and D. Stroud, "Effective dielectric response of nonlinear composites," *Physical Reviw B*, vol. 47, pp. 14150-14156, 1993.

[80] A. Sihvola, "Self-consistency aspects of dielectric mixing theories," *IEEE Trans. Geosci. Remote Sensing*., vol. 27, pp. 403–415, July 1989.

[81] B. Jia, W. Lin and S. Liu, "The study of effective medium parameters for granular media," *Prog. Electromagn. Res*., vol. 8, pp. 89-108, 1994).

[82] C. Chevigny, D. Gigmes, D. Bertin, J. Jestin, and F. Boué, "Polystyrene grafting from silica nanoparticles via nitroxide-mediated polymerization (NMP) : synthesis and SANS analysis with the contrast variation method," *Soft Matter*, 5(19), pp. 3741–3753, 2009.

[83] A. Brulet, F Lafuma, L. Petit, L. Bouteiller and D. Hourdet, "Responsive hybrid selfassemblies in aqueous media," *Langmuir*, vol. 23, pp. 147–158, 2007.

[84] A. Vial and T. Laroche, "Comparison of gold and silver dispersion laws suitable for FDTD simulations," *Appl. Phys. B-Lasers Opt.*, vol. 93, pp. 139-143, 2008.

[85] V. Myroshnychenko and C. Brosseau, "Finite-element method for calculation of the effective permittivity of random inhomogeneous media," *Phys. Rev. E*., vol. 7, pp. 016701-016716, 2005.

[86] N. Jebbor and S. Bri, "Effective permittivity of periodic materials: Numerical modeling by the finite element method," *J. of Electrostatics*, vol. 70, pp. 393-399, 2012.

[87] B. Sareni, L Krähenbühl, A. Beroual, and C. Brosseau, "Effective dielectric constant of periodic composite materials," *J. Appl. Phys.*, vol. 80(3), pp. 1688-1696, 1996.

[88] K. Ghosh and M. E. Azimi, "Numerical calculation of effective permittivity of lossless dielectric mixture using Boundary Integral Method," *IEEE Trans. on Diel. and Elect. Insul.*, vol. 1, pp. 975- 981, 1994.

[89] G. Weick, R.A. Molina, D. Weinmann and R.A. Jalabert, "Lifetime of the first and second collective excitations in metallic nanoparticles," *Phys. Rev. B*, vol. 72, pp. 115410-1-17, 2005.

[90] E.D. Palik, *Handbook of Optical Constants of Solids III*, Academic Press, New York, 1991.

[91] W. Rechberger, A. Hohenau, A. Leitner, J.R. Krenn, B. Lamprecht and F.R. Aussenegg, "Optical properties of two interacting gold nanoparticles," *Optics Communications*,vol. 220, pp. 137–141, 2003.

[92] A.R. Senoudi , F. Lallam , A. Boussaid , M. Benhamou, "Numerical Study Of The Effects Of Polymeric Shell On Plasmonic Resonance Of Nanogolds," *International Journal Of Academic Research*, vol. 2 (3), pp. 70-78, 2010.

[93] C. Durand-Gasselin, M. Capelot, N. Sanson, and N. Lequeux, "Tunable and reversible aggregation of poly(ethylene oxide-st-propylene oxide) grafted gold nanoparticles," *Langmuir*, vol. 26(14), pp. 12321_12329, 2010.

[94] C. Durand-Gasselin, N. Sanson, and N. Lequeux, "Reversible controlled assembly of thermosensitive polymer-coated gold nanoparticles," *Langmuir*, vol. 27(20), pp. 12329-12335, 2011.

